2024 IEEE 4th International Maghreb Meeting of the Conference on Sciences and Techniques of Automatic Control and Computer Engineering (MI-STA),Tripoli, Libya, 19-21 May 2024.

Control Technique of MPPT Utilizing for Boost Converter Applied to Small Renewable Energy System and a DC Microgrid for Remote Area

Ahmed Zentani
Department of Electrical Electronics and Computer Engineering
Cape Peninsula University of Technology
Cape Town, South Africa
217001882@mycput.ac.za

Ali Almaktoof
Department of Electrical Electronics and Computer Engineering
Cape Peninsula University of Technology
Cape Town, South Africa
almaktoofa@cput.ac.za

M.T.E Kahn
Department of Electrical Electronics and Computer Engineering
Cape Peninsula University of Technology
Cape Town, South Africa
khant@cput.ac.za

***Abstract*— The growing concerns about the environment, depletion of fossil fuels, and increasing energy consumption have led to a rise in the adoption of renewable energy sources. However, integrating these green energy sources into the existing power system requires infrastructure modifications. One popular approach is the establishment of off-grid operations through the use of microgrids. Microgrids are small-scale power systems that can operate both connected to and disconnected from the main power grid. This study focuses on a DC microgrid that utilizes a renewable energy system to power DC loads in case of a conventional grid failure. The system incorporates various components such as a universal diode rectifier, a boost converter, a small wind turbine (SWT) connected to a permanent magnet synchronous generator, and the Incremental Conductance (IC) algorithm. These components are employed to maximize the output power of the boost converter and maintain precise control over the output voltage, ensuring reliability. To efficiently operate the switching element and achieve a fast Maximum Power Point Tracking (MPPT) technique and voltage regulation despite varying wind speeds, a modified IC MPPT control method is utilized. A MATLAB/Simulink model representing an SWT system for a DC microgrid is developed to assess the dependability of the proposed system under changing wind speeds.**

Keywords*— DC microgrids, Boost converters, IC MPPT algorithm, a renewable energy source of small wind turbine.

I. Introduction

Currently, energy scarcity is a pressing issue faced by many nations. In some cases, these nations implement restrictions on household electricity usage [1], [2]. While the cost of electricity from traditional grids continues to rise. To combat this, small renewable generators are increasingly being installed in homes and businesses to reduce energy costs and carbon dioxide emissions and even sell excess electricity back to utility grids. These generators serve as backup sources to maintain a steady electricity supply during power outages [3]. Among various renewable generators, wind turbines are recognized as one of the cleanest and most efficient technologies available, with sizes varying depending on the intended purpose [4]. Small off-grid wind turbines have become an appealing option for supplying electricity to residential areas, especially during grid failures, power outages, or in remote locations without access to national grids. Unlike large wind turbines commonly found in wind farms, medium and small-scale wind turbines can be installed in more flexible environments. For example, small wind turbines (SWTs) are frequently used in urban distributed energy networks to supply direct current (DC) or alternating current (AC) electricity. This study focuses on residential utilities, such as DC appliances (e.g., LED lighting, laptops, variable speed drives), which significantly contribute to increased electricity demand in homes. DC microgrids offer several advantages, including enhanced energy efficiency, reduced total energy consumption, operational benefits, and cost-effective power infrastructure replacement [5]. Recent research has revealed that DC microgrids outperform AC microgrids in terms of various benefits, including higher reliability, improved power quality, reduced losses due to reactive power, simplified design, and enhanced performance and efficiency of DC converters [6]: higher dependability, better quality power supplies, reduced losses due to reactive power, simple design, and DC converters with improved performance and efficiency.

The performance of a wind generator in terms of power production depends on the accuracy of its Maximum Power Point Tracking (MPPT) controller, which determines the highest power points to operate at [7]. MPPT algorithms are commonly used in renewable energy systems, such as photovoltaic and wind turbines, to maximize output power under various operating conditions [8]. Numerous MPPT algorithms have been described in the literature, with conventional methods utilizing mechanical parameters like wind turbine speed to calculate maximum power (torque) or maintain optimal generator speed values for different wind speeds [9]. The most widely used gearless standalone SWT designed for use in isolated areas is a permanent magnet synchronize generator (PMSG). A system contains a boost converter attached to a universal rectifier that is managed by an IC MPPT controller. This study-implemented DC microgrid off-grid has a renewable source supply of 3.9 KW and 270 VDC to the load, which is controlled by an incremental conductance (IC) controller method.

The rest of the paper is structured as follows. The study methodology used for this project is presented in Section II. Section III presents the results and discussions. The major research conclusions of this paper are finally summarized in Section IV.

II. Research Method

The use of DC microgrid technologies is increasingly popular in various commercial applications, such as data centers, telecom hubs, fast electric vehicle (EV) charging stations, railroads, and electric ships. To gain a comprehensive understanding of the current landscape and practical implementations of DC microgrid technologies in different commercial sectors, Fig. 1 illustrates the structure of a DC microgrid composed of multiple nano-grids. This visualization aids in comprehending the hierarchical organization of the microgrid and the distribution of power and control among its various components.

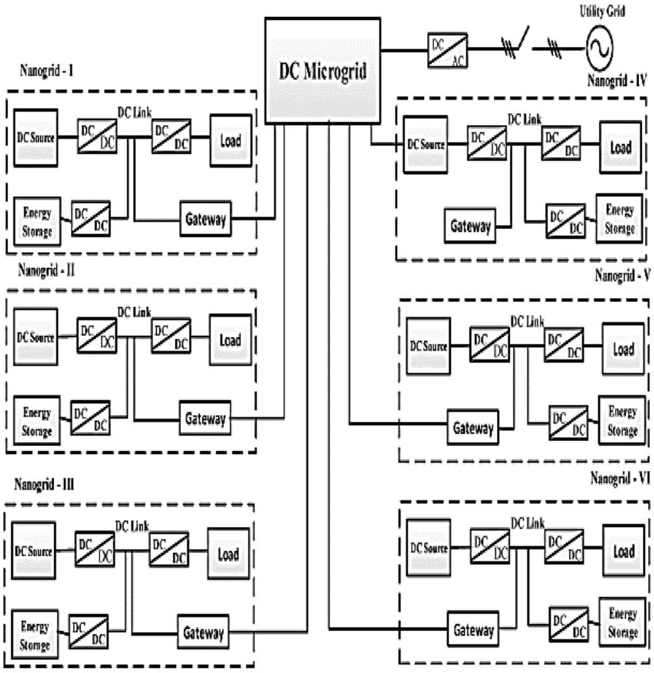

Fig. 1. Nano-grids forming a DC microgrid [10].

Fig. 2 presents a DC off-grid system specifically designed for a wind turbine as the power source. The system comprises three main parts: the wind turbine source, a power conditioning converter, and an IC control module responsible for regulating the power transferred from the source to the load. Fig. 2 provides a visual representation of the system described in this study.

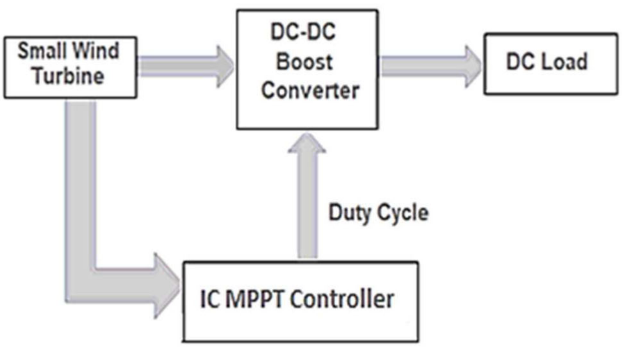

Fig. 2. Small wind used to DC off grid.

A. Source of small wind turbine

Fig. 3 visually represents the power curve of a wind turbine, illustrating the relationship between its rotor rotational speed and various wind speeds. The curve demonstrates the cubic power dependency of the wind turbine on wind speed, highlighting its capacity to achieve maximum power generation based on the rotation speed.

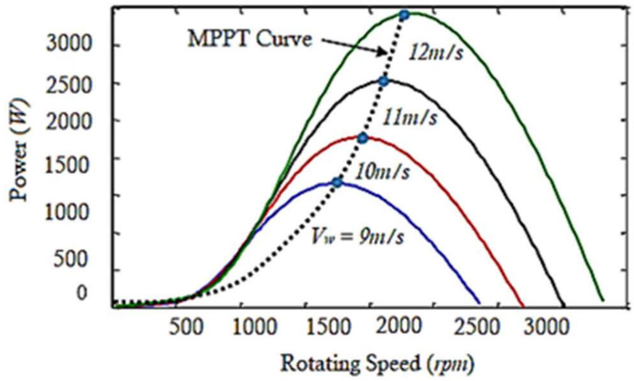

Fig. 3. Power versus rotor rotational speed at various rotational wind speeds [10].

The rotor blades of the wind turbine convert the wind's kinetic energy into mechanical energy. This mechanical energy is then converted into electrical energy through an electric generator connected to the rotor. The extraction of wind energy occurs at different rotational speeds depending on the structure and shape of the blades. In general, the wind turbine is capable of extracting maximum power from the wind even under fluctuating wind conditions.

$$E = \frac{1}{2}\rho A C_p V_w^3 \qquad (1)$$

Where A is the cross-sectional air volume of the rotor, ρ is the air density, and V_w is the turbine speed. The models can transform into equivalent circuitry using a two-axis frame. The $dq0$ axis shown in this part serves as a demonstrated of the generator's stator and rotor windings. The voltage of the permanent magnet synchronization generator in the $dq0$ reference frame is given by the equations below. (2) and (3).

$$v_d = R_d i_d + L_d \frac{di_d}{dt} - \omega_e \psi q, \qquad (2)$$

$$v_q = R_q i_q + L_q \frac{di_q}{dt} + \omega_e \psi d, \qquad (3)$$

The current generator is represented by i_d and i_q at d axis and$q$axis, whereas the rotor resistance is represented by R_d and R_q at d axis and q axis, whereas ψ_{PM} represents the magnet flux and ω_e is the generator's rotational speed.

B. DC-DC Boost converter design

The depicted boost converter in Fig. 4 accepts a DC input voltage and produces an output voltage that is higher than the input. Typically, this converter comprises components such as an inductor, a diode, a switch, and at least one energy storage element. Capacitors are often connected to the converter's output terminal to mitigate any voltage fluctuations. When the switch, typically an insulated-gate bipolar transistor (IGBT), is in the on-state mode, the current flowing through the inductor increases. Conversely, when the switch is in the off-state mode, the only path for the inductor current is through the diode, capacitor, and load. This arrangement allows the capacitor to transfer the energy stored during the on-state mode. The output voltage V_o of a boost converter can be determined using equation 5, as stated below [11]:

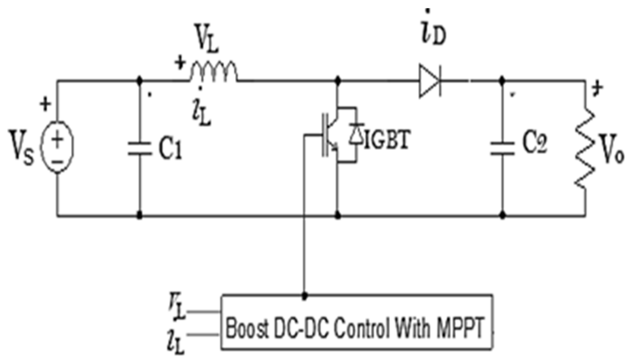

Fig. 4. Incremental conductance controller used in boost converter.

To maximize power while the wind speed is variable, the converter switch's control must be used to regulate the generator speed of the turbine. The IC MPPT algorithm method is used in this case to regulate the converter due to its simplicity of implementation. The duty ratio is adjusted to use the maximum amount of power extracted to provide the necessary voltage. P_w the power output written as:

$$P_w = V_w \ I_w, \tag{4}$$

V_w and I_w where set of small wind turbines. Equation (5) describe the system relationship between voltage V_w and DC link voltage V_{dc}:

$$V_w = \left(\frac{1}{1-D}\right) V_{dc}, \tag{5}$$

Most boost converters are designed to function with a continuous current. Equation (6) gives the inductance to generate constant current, while Equations (8) and (12) depict the voltage ripple. High as switching frequencies increase, inductor and capacitor minimum sizes for generating continuous current and limiting output ripple, respectively, both decreases, allowing for smaller inductor and capacitor sizes. However, high switching frequencies result in increased power loss in the switches and reduced converter effectiveness.

By comparing the inductor current and voltage of boost converter switch closed and open relate to one another, it is determined in Fig. 5.

The diode is reverse-biased when the circuit is closed, as shown in Fig. 5c, and the Kirchhoff voltage equation expressed as follows:

$$V_S = L\frac{di_L}{dt}. \tag{6}$$

The current rise linearly because the rate of current variation is constant. Equations (7) and (8) represent the variation in inductor current as

$$\frac{\Delta i_L}{\Delta t} = \frac{\Delta i_L}{DT} = \frac{V_S}{L}, \tag{7}$$

$$(\Delta i_L)_{closed} = \frac{V_S DT}{L} \tag{8}$$

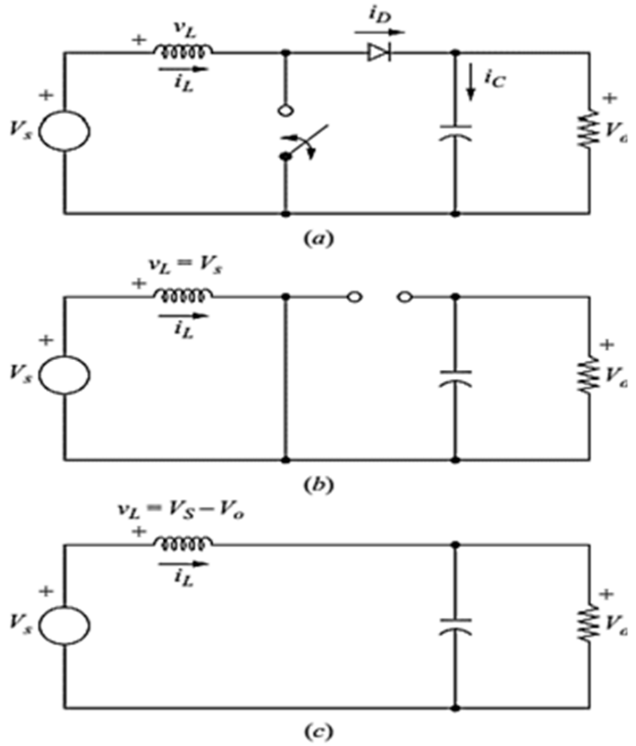

Fig. 5. The boost converter. (a) Circuit; (b) circuit switch is closed; (c) circuit switch is open.

The inductor current cannot change instantly when the circuit is open. The diode is proceeding-biased and the voltage across the inductor and the variation of the inductor current are provided as follows:

$$v_L = V_S - V_O = L\frac{di_L}{dt}, \tag{9}$$

$$\frac{di_L}{dt} = \frac{V_S - V_O}{L}. \tag{10}$$

Since the rate of inductor current fluctuation is constant, the switch remains open even as current changes linearly. The variations inductor current (11) and (12) as follows [12]:

$$\frac{\Delta i_L}{\Delta t} = \frac{\Delta i_L}{(1-D)T} = \frac{V_S - V_O}{L}, \tag{11}$$

$$(\Delta i_L)_{open} = \frac{(V_S - V_O)(1-D)T}{L}. \tag{12}$$

In steady-state conditions, the inductor current's net variation is equal to zero, and the converter's output voltage is provided as follows:

$$V_O = \frac{V_S}{1-D}. \tag{13}$$

Where output voltage goes toward infinity as the switch's duty ratio approaches unity to 1. However, real components are always subject to losses that prevent this from happening.

C. Incremental conductance method control strategy

The incremental conductance technique is a common MPPT algorithm which consists of ascertaining the optimum point by making a correlation between current conductance $\frac{I}{V}$ with the incremental conductance $\left(\frac{dI}{dV}\right)$ and continues knowing that the slope of power versus voltage characteristic is zero at maximum power point and that the power is given as the product of the current and the voltage. The incremental conductance method is defined by the following equations (14):

$$\left(\frac{dP}{dV}\right) mpp = \frac{d(VI)}{dV} \quad (14)$$

$$I + V\left(\frac{dI}{dV}\right) mpp = 0 \quad (15)$$

$$\left(\frac{dI}{dV}\right) mpp = -\frac{I}{V} \quad (16)$$

Equation 16 represents the principal condition to realize the maximum power point, when the variance of the output conductance is equal to the negative of the output conductance. The flowchart of the incremental conductance method is depicted in Fig. 6.

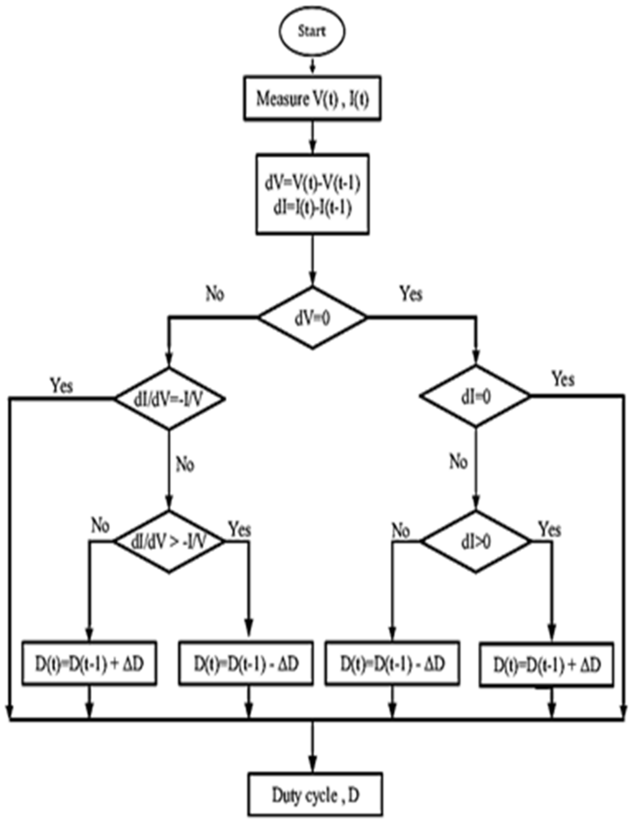

Fig 6. Flowchart of incremental conductance algorithm for SWT used to boost converter.

A boost converter using an IC technique for off-grid DC power. The MPPT controller receives measured voltage and current as inputs. Then, in order to monitor the ideal output power, the IC algorithm is applied to these variables. The boost converter uses the signal produced by the IC controller technique as input to sustain the MPPT voltage by varying the duty ratio. A small signal disorder that affected the system's AWT power was present. Uncertainty the disorder cause to increase limit of power then will continue the same track. When the power reaches its peak, it decreases the following instant, and the disorder indication signal reverses. During steady state, the MPP is subject of the oscillate algorithm. Variation power is minimized by possession of the disorder size small.

The flowchart of the developed algorithm is shown in Fig. 4. The adopted control method ensures effective speed management control to extract the optimum output power. The system disorder voltage is a slight increase of dV, resulting during a change in dI/dV. If dI/dV positive, the voltage disorder a maintained comparable direction as the slight increase. Conversely, assuming when dI/dV negative, the shift points from MPP, while changing voltage, should change on the contrary side during a small increase.

Any alteration in the duty ratio will have an inverse impact on the boost converter's input resistance, which will have an inverse impact on the operating voltage. The algorithm technique then determines the suitable command for the subsequent cycle by examining how changing the duty cycle has an impact on the output power. Raising the voltage, for instance, could increase the total power. Therefore, the algorithm in the subsequent cycle will cause a rise in voltage, which may be accomplished by reducing the duty cycle.

III. Results And Discussion

Consequently, the diode rectifier is employed to convert the variable AC voltage and current from the wind turbine into a DC voltage. This rectification process is followed by a boost converter that elevates the voltage to a regulated DC level suitable for the load requirements. The gradual inductance MPPT controller utilizes the same input source as the boost converter. The converter's input voltage and current are continuously utilized to calculate the duty ratio and supply the boost converter. The MPPT technique adjusts the voltage of the boost converter based on the duty ratio to consistently track the optimal power point. Ultimately, the resistive load outcome represents the power demand for the DC microgrid. The specific values for the application parameters are detailed in Table I.

TABLE I. Windwind Turbine And Boost Converter System Parameters.

Description	***Rating***
Rated Power, *P*	3.9 KW
Input Voltage, V_{in}	130 V
Output Voltage, V_{out}	270 V
Inductance current, *L*	1.263x10^{-3}H
Switching Frequency, *fs*	5 KHz
DC Link capacitors, *C*	210.4 μF
Peak inductor current	0.3 A
Resistance load, *R*	20Ω
Capacitance ripple	0.01 %
Voltage ripple	0.04 %
Sample time, *Ts*	50x10^{-5} *s*

The converter's 130 VDC and 3.9 KW diode rectifier inputs. The inductance current of the boost converter is shown in Fig. 7 where the figure depicts significant fluctuations at the beginning of the simulation until time of 0.32 seconds before the system becomes stable. A maximum current of 36.2 A respectively. Signal steady state rating of 28.9 A.

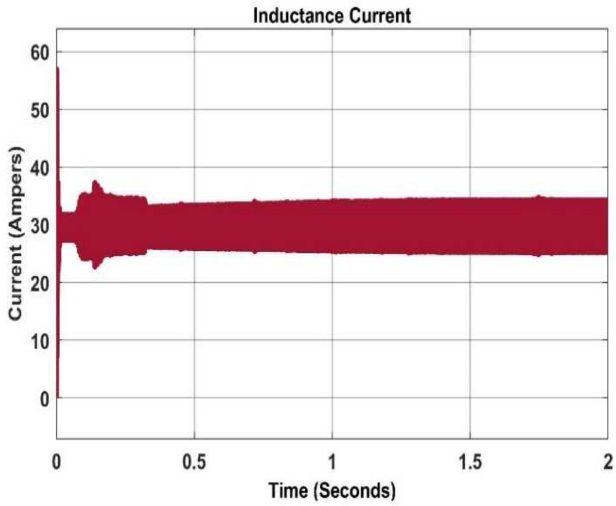

Fig. 7. Inductance current of boost converter.

Fig. 8 illustrates the output voltage rectifier's steady state at around 130V; the signal showed an overshoot of 0.909% and undershoot before stable is 2%, and it took approximately 0.07 s to achieve a steady state value.

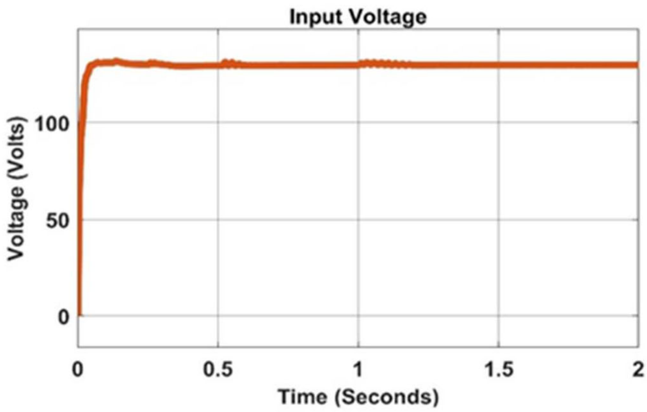

Fig 8. Input voltage of boost converter.

Fig. 9 displys that the converter rise time is 22.631 ms and shows an overshoot value of 2.178% and an undershoot value of 4.387%. Current increased to 10 A at 7 m/s speed variation operating between t = 0.5 and t = 0.7 s, and at 11 m/s speed variation operating between t = 1.05 and t = 1.3 s, current fluctuation by varying speed then reached a stability value of 14.38 A.

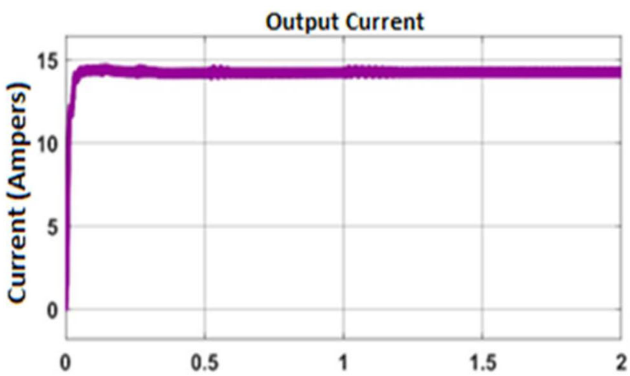

Fig 9. Output current of boost converter.

Fig. 10 shows the output voltage of the converter. The rise time is displayed as 22.658 ms. At t = 0.3 s, the voltage stabilized at 270 VDC, and the duty cycle increased to 0.628, which corresponds to a wind speed of 12 m/s.

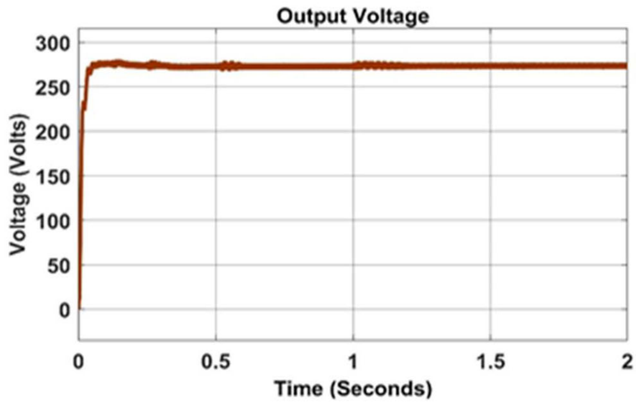

Fig 10. Output voltage of boost converter.

Fig. 11 shows the output power with rise times of 22.658 ms and 8.387% undershoot respectively. Fluctuation at various times based on changing speed. The rated power (3.9 kW) with the required turbine speed (12 m/s) were both attained at t = 0.23 s.

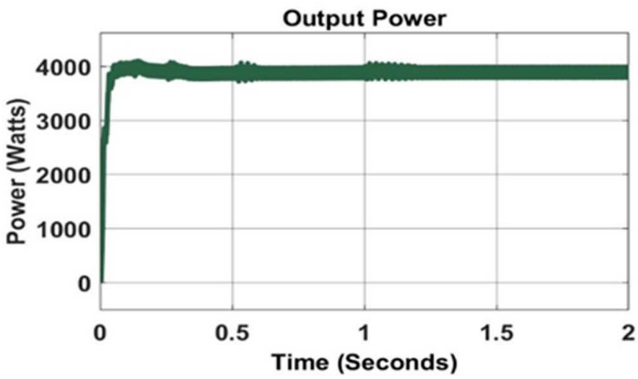

Fig 11. Output power of boost converter.

IV. Conclusion

The focus of this research study was to develop a model of a DC microgrid that utilizes An SWT to supply DC power during load shedding situations. The research conducted simulations to analyse and discuss the performance of the system. One key aspect of the system addressed the control of the boost converter's output, which was achieved through incremental control based on the results of the SWT system. The simulations carried out to ensure that the SWT permanent magnet synchronous generator produced an output of 3.9 kW are simulated. Additionally, the boost converter is designed to meet the demand of 270 VDC to supply power to the microgrid. The research focused on developing to optimize the performance and maintain a constant voltage level in the application of the turbine system and DC microgrid model, the incremental conductance algorithm controller was used to achieve the best tracking value for the system to ensure a stable voltage output and maintain a reliable power supply to the microgrid.

REFERENCES

[1] O. M. Akinbami, S. R. Oke, and M. O. Bodunrin, "The state of renewable energy development in South Africa: An overview," *Alexandria Eng. J.*, vol. 60, no. 6, pp. 5077–5093, 2021, doi: 10.1016/j.aej.2021.03.065.

[2] M. Kesraoui, N. Korichi, and A. Belkadi, "Power Management of a Hybrid Wind Gas Electrolyze Micro grid," *Int. Renew. Energy Congr.*, no. Irec, 2018.

[3] M. Kesraoui, N. Korichi, and A. Belkadi, "Maximum power point tracker of wind energy conversion system," *Renew. Energy*, vol. 36, no. 10, pp. 2655–2662, 2011, doi: 10.1016/j.renene.2010.04.028.

[4] J. EARNEST and S. RACHEL, *Wind Power Technology*, Third Edit., vol. 35, no. 9. Delhi: Asoke K. Ghosh, PHI Learning Private Limited, Rimjhim House, 2019. doi: 10.1088/0031-9112/35/9/023.

[5] R. Usman, P. Mirzania, S. W. Alnaser, P. Hart, and C. Long, "Systematic Review of Demand-Side Management Strategies in Power Systems of Developed and Developing Countries," *Energies*, vol. 15, no. 21, pp. 1–24, 2022, doi: 10.3390/en15217858.

[6] M. Zolfaghari, G. B. Gharehpetian, M. Shafie-khah, and J. P. S. Catalão, "Comprehensive review on the strategies for controlling the interconnection of AC and DC microgrids," *Int. J. Electr. Power Energy Syst.*, vol. 136, no. November 2020, 2022, doi: 10.1016/j.ijepes.2021.107742.

[7] X. C. Le, M. Q. Duong, and K. H. Le, "Review of the Modern Maximum Power Tracking Algorithms for Permanent Magnet Synchronous Generator of Wind Power Conversion Systems," *Energies*, vol. 16, no. 1, 2023, doi: 10.3390/en16010402.

[8] L. Bhukya, N. R. Kedika, and S. R. Salkuti, "Enhanced Maximum Power Point Techniques for Solar Photovoltaic System under Uniform Insolation and Partial Shading Conditions: A Review," *Algorithms*, vol. 15, no. 10, 2022, doi: 10.3390/a15100365.

[9] D. R. Lopez-Flores, J. L. Duran-Gomez, and M. I. Chacon-Murguia, "A Mechanical Sensorless MPPT Algorithm for a Wind Energy Conversion System based on a Modular Multilayer Perceptron and a Processor-in-the-Loop Approach," *Electr. Power Syst. Res.*, vol. 186, no. May, p. 106409, 2020, doi: 10.1016/j.epsr.2020.106409.

[10] J. Kumar, A. Agarwal, and V. Agarwal, "A review on overall control of DC microgrids," *J. Energy Storage*, vol. 21, pp. 113–138, 2019, doi: 10.1016/j.est.2018.11.013.

[11] R. Aubrée, F. Auger, and P. Dai, "A new low-cost sensorless MPPT algorithm for small wind turbines," *2012 1st Int. Conf. Renew. Energies Veh. Technol. REVET 2012*, no. March, pp. 305–311, 2012, doi: 10.1109/REVET.2012.6195288.

[12] W. Hart Danial, *Power Electronics*. Indiana: McGraw-Hill, 2011.